BRAIN RESEARCH 1374 (2011) 43–55

available at www.sciencedirect.com

ScienceDirect

www.elsevier.com/locate/brainres

BRAIN RESEARCH

Research Report

Comparative neuroanatomical and temporal characterization of FluoroJade-positive neurodegeneration after status epilepticus induced by systemic and intrahippocampal pilocarpine in Wistar rats

O.W. Castro, M.A. Furtado[1], C.Q. Tilelli[2], A. Fernandes, G.P. Pajolla, N. Garcia-Cairasco*

Physiology Department, Ribeirão Preto School of Medicine, University of São Paulo, Ribeirão Preto, São Paulo, Brazil

ARTICLE INFO

Article history:
Accepted 4 December 2010
Available online 11 December 2010

Keywords:
Neuronal damage
Status Epilepticus
Behavioral analysis
Limbic system

ABSTRACT

The aims of this study were to characterize the spatial distribution of neurodegeneration after status epilepticus (SE) induced by either systemic (S) or intrahippocampal (H) injection of pilocarpine (PILO), two models of temporal lobe epilepsy (TLE), using FluoroJade (FJ) histochemistry, and to evaluate the kinetics of FJ staining in the H-PILO model. Therefore, we measured the severity of behavioral seizures during both types of SE and also evaluated the FJ staining pattern at 12, 24, and 168 h (7 days) after the H-PILO insult. We found that the amount of FJ-positive (FJ+) area was greater in SE induced by S-PILO as compared to SE induced by H-PILO. After SE induced by H-PILO, we found more FJ+ cells in the hilus of the dentate gyrus (DG) at 12 h, in CA3 at 24 h, and in CA1 at 168 h. We found also no correlation between seizure severity and the number of FJ+ cells in the hippocampus. Co-localization studies of FJ+ cells with either neuronal-specific nuclear protein (NeuN) or glial fibrillary acidic protein (GFAP) labeling 24 h after H-PILO demonstrated spatially selective neurodegeneration. Double labeling with FJ and parvalbumin (PV) showed both FJ+/PV+ and FJ+/PV− cells in hippocampus and entorhinal cortex, among other areas. The current data indicate that FJ+ areas are differentially distributed in the two TLE models and that these areas are greater in the S-PILO than in the H-PILO model. There is also a selective kinetics of FJ+ cells in the hippocampus after SE induced by H-PILO, with no association with the severity of seizures, probably as a consequence of the extra-hippocampal damage. These data point to SE induced by H-PILO as a low-mortality model of TLE, with regional spatial and temporal patterns of FJ staining.

* *Corresponding author*. University of São Paulo, Ribeirão Preto School of Medicine, Av.Bandeirantes, 3900, Ribeirão Preto 14049-900, SP, Brazil. Fax: +55 16 3633 0017.
E-mail address: ngcairas@fmrp.usp.br (N. Garcia-Cairasco).
[1] Current address: Walter Reed Army Institute of Research, Silver Spring, MD, USA.
[2] Current address: Federal University of São João del Rei. Campus Centro-Oeste Dona Lindu, Divinópolis, MG, Brazil.

0006-8993
doi:10.1016/j.brainres.2010.12.012

1. Introduction

Status Epilepticus (SE) is defined as a condition in which an uninterrupted seizure or several epileptic seizures occur repeatedly, without recovery, for a period of 30 min or more. This period of seizures leads to a chronic epileptic state (Shorvon, 2000). In TLE patients (with generalized convulsive SE, not with complex partial SE) and in animal models, SE is usually associated with cell loss throughout the brain. In particular, the hippocampus shows selective degeneration of interneurons in the *hilus* of the dentate gyrus (DG) and of pyramidal neurons in *cornus ammoni* subfields such as CA1 and CA3 (Mohapel et al., 2004). Degeneration is also observed in many other areas, such as amygdala, thalamus, olfactory cortex, neocortex, and substantia nigra (Fujikawa, 1996, 2005; Turski et al., 1987). We recently developed a model of SE induced by intra-hippocampal microinjection of pilocarpine (H-PILO) (Furtado et al., 2002). This model mimics acute and chronic behavioral, electroencephalographic and morphological aspects of TLE and also has a low-mortality profile.

The purpose of this study was to identify FluoroJade (FJ)-positive (FJ+) neurodegeneration (Schmued et al., 1997) 24 h after SE induced by H-PILO and to compare this pattern of neurodegeneration to that which is observed in the most commonly used model for TLE, the systemic PILO model (S-PILO). Furthermore, we evaluated FJ+ neuronal damage at 12, 24 and 168 h (7 days) after SE in the H-PILO model in order to verify the regional distribution and kinetics of the neurodegeneration process. Finally, we evaluated a potential relationship between the FJ+ neurodegeneration pattern and the severity of behavioral seizures during SE.

2. Results

In spite of similar features of behavioral SE when comparing S-PILO AND H-PILO groups (data not shown; see discussion on characteristics of the H-PILO model in Furtado et al., 2002), we identified a differential distribution of neurodegenerating areas. Table 1 shows a comparison between H-PILO and

Table 1 – Mapping FJ-positive neurons in the S-PILO (S) and H-PILO (H) models of TLE.

Area	Sub-area	Group	
Cortex	Retrosplenial	S	H
	Auditory, layer II	S	H
	Auditory, layer III	S	H
	Auditory, layer IV		H
	Entorhinal, layers II	S	H
	Entorhinal, layer IV	S	H
	Entorhinal, layer V	S	H
	Entorhinal, layer VI	S	H
	Piriform, layer II	S	H
	Piriform, layer III	S	H
	Temporal-associative	S	H
	Insular	S	H
Endopiriform nucleus		S	H
Amygdaloid complex	Cortical nucleus	S	H
	Basomedial nucleus	S	H
	Lateral nucleus	S	H
	Central nucleus	S	
	Amygdalo–hippocampal transition area	S	H
Hippocampus	Hilus	S	H
	CA3 pyramidal	S	H
	CA2 pyramidal	S	
	CA1 pyramidal	S	H
	Subiculum	S	H
	Stratum oriens	S	
Thalamus	Lateral posterior thalamic nucleus	S	
	Zona incerta	S	
	Dorsal lateral geniculate nucleus	S	
	Paraventricular thalamic nucleus	S	
	Mediodorsal thalamic nucleus, lateral	S	
	Mediodorsal thalamic nucleus, central	S	
	Mediodorsal thalamic nucleus, medial	S	H
	Posteromedial thalamic nucleus	S	
	Reuniens	S	H
	Ventrolateral thalamic nucleus, laterodorsal		H
	Centrolateral thalamic nucleus		H
Hypothalamus	Medial tuberal nucleus	S	
	Premamillary nucleus	S	

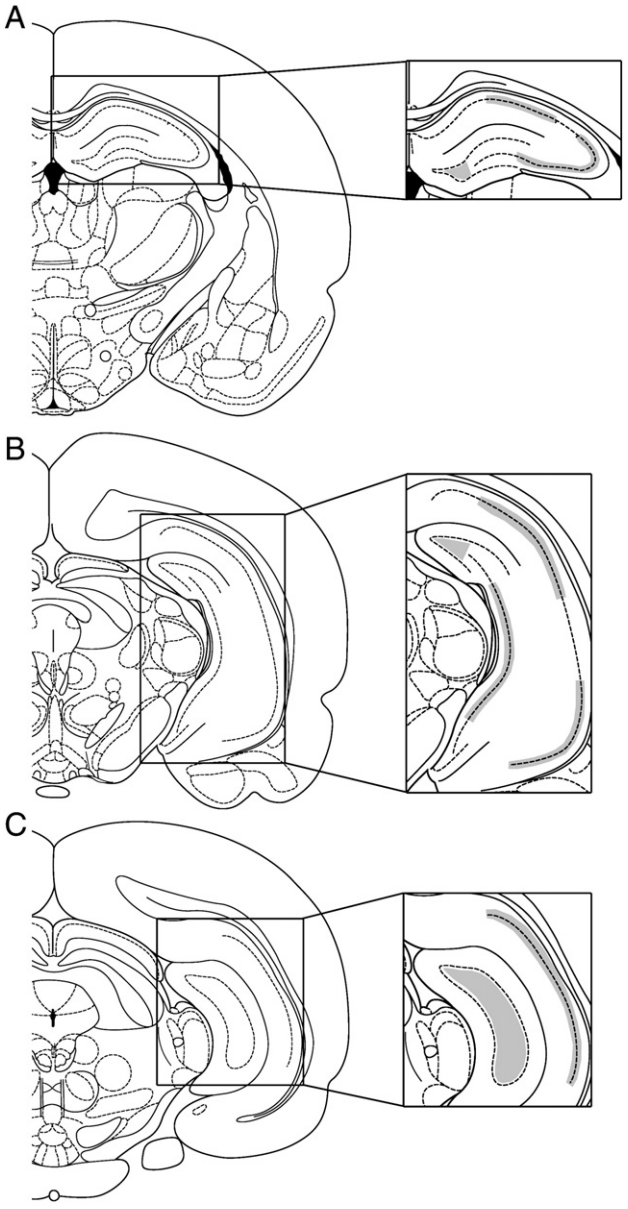

Fig. 1 – Representation of regions sampled to count FJ-positive cells (Paxinos and Watson, 1996).

S-PILO models concerning FJ+ cell-containing regions. Thirty-seven regions contained FJ+ cells, of which 3 were seen exclusively in the H-PILO group, 12 were exclusively seen in the S-PILO group, and 22 were seen in both groups. Note that seven thalamic and two hypothalamic nuclei, as well as the central nucleus of the amygdala, are exclusively affected by S-PILO. On the other hand, H-PILO, with significantly fewer damaged areas, also presents a differential pattern involving two thalamic nuclei and auditory cortical layer IV.

In the H-PILO group, 28 of 36 (78%) injected animals had SE, and most of those animals survived (97%). Among the animals that underwent SE, 21% had predominantly class 1 seizures (group A), 18% had class 2 (group B), 34% had class 3 (group C), 24% had class 4 (group D) and 3% had class 5 seizures (group E). These results are represented in Fig. 2. The latency to SE was 19±9 min (mean±SEM). Shortly after H-PILO microinjection,

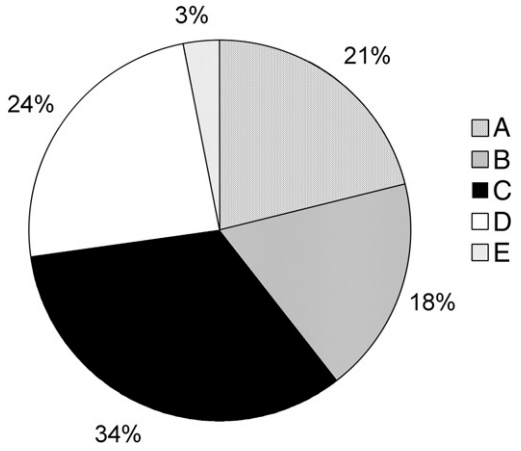

Fig. 2 – Distribution of behavioral seizures in H-PILO model (A–E), based on the seizure severity index of Pinel and Rovner (1978).

the animals that presented SE showed facial automatisms associated with moderate salivation and piloerection. Fifteen to 30 min after SE onset, animals usually progressed to limbic motor seizures (eyes blinking, chewing behavior, head nodding, forelimb myoclonus, rearing, and falling).

There was no correlation between seizure severity and number of FJ+ cells in any subregion of the hippocampal formation in all time points studied (Pearson's correlation test, $P<0.05$). However, taking into account the region and the time post-SE, we observed that the number of FJ+ cells declines as a function of time in the DG hilus. In fact, there is a statistically significant difference only between the 12 h and 168 h groups as shown in Fig. 3. On the other hand, in CA3, FJ+ cell number increases from 12 to 24 h and stabilizes at 168 h. In addition, CA1 contains more neurodegenerating cells for the longest time post-SE when compared with 12 and 24 h groups (Kruskal–Wallis one-way ANOVA with post-hoc Dunn's: $P<0.01$; results expressed as mean±SEM, Fig. 3). We did not find neurodegeneration in control animals. In fact, in these animals, we only detected a small mechanical lesion caused

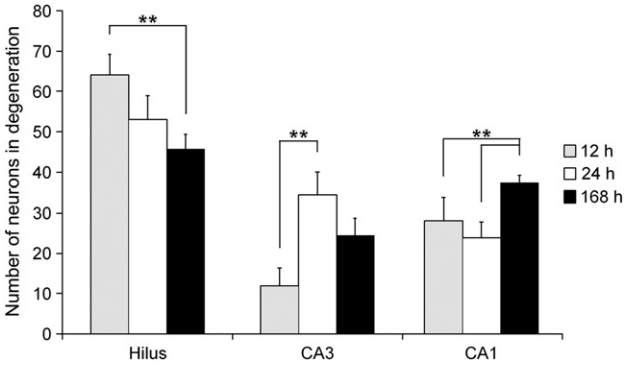

Fig. 3 – Cell Loss in selective hippocampal regions at specific time points after SE in H-PILO model. The DG *hilus* presented higher neurodegeneration 12 h after SE. The CA3 region presented higher pattern of neurodegeneration 24 h after SE, and the CA1 region presented higher cell loss 168 h after SE. Kruskal–Wallis one-way with Dunn's post-hoc test; $^{**}p<0.01$.

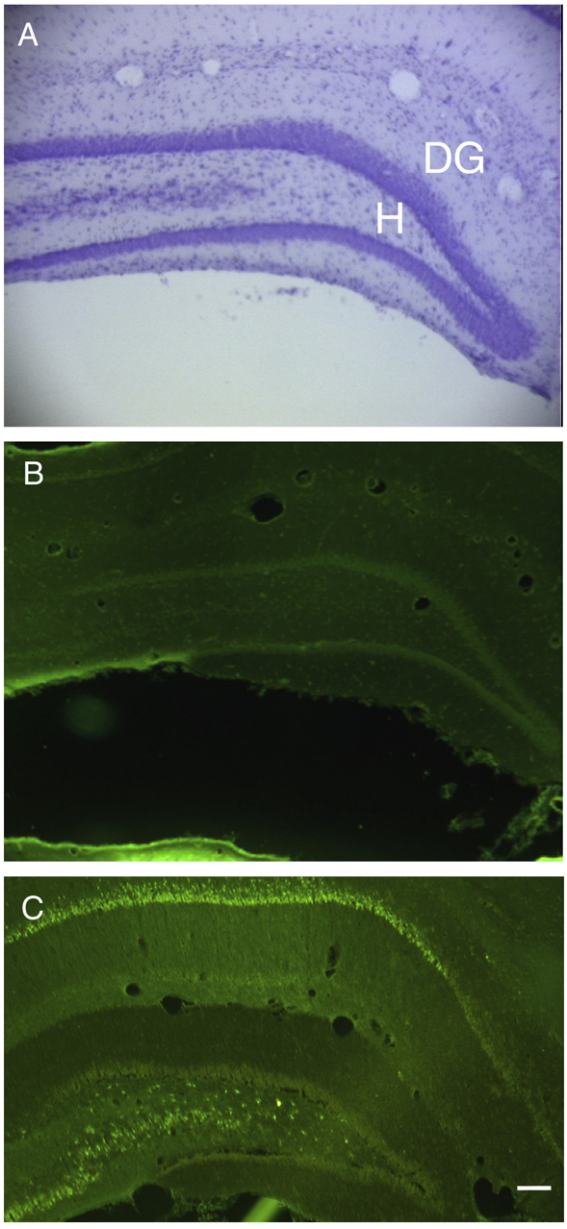

Fig. 4 – Example of histology in Control (A, Nissl staining; B and C, FJ staining) and H-PILO (C, FJ staining) groups. Control animal was sacrificed 24 h after vehicle microinjection. Note the absence of FJ+ cells in the control tissue and FJ+ cells in experimental tissue in C. H, *hilus*; DG, granular cells of the DG. Calibration bar = 500 μm.

by the cannula. An example of the contrasting findings between control and H-PILO groups can be visualized in Fig. 4. However, in all animals that went into SE, we observed an extensive FJ+ response in CA1, CA3, and DG hilus (Fig. 5). We also observed FJ+ staining in other areas, such as cortical regions, amygdala, and thalamus (data not shown).

FJ/NeuN double staining in Fig. 6 showed a partial FJ/NeuN co-localization in wide areas of the hilus (Fig. 6A) and CA3 (Fig. 6C). These experiments also demonstrated very selective laminar labeling showing preserved (NeuN+) CA1 neurons (Fig. 6B) in regions that lack FJ (stratum oriens/stratum pyramidale transition), and another lamina with very weak NeuN labeling in regions with strong FJ labeling (Fig. 6B′; stratum pyramidale/stratum radiatum transition). Notice in the merged image (Fig. 6B″) the exact correspondence between preserved lamina (dorsal) and neurodegenerated lamina (ventral). All these images are representative of the H-PILO model. Fig. 7 shows typical photomicrographs in the hilus, CA1, and CA3 showing the partial co-localization of FJ+ cells with GFAP.

We found various combinations of FJ/PV labeling in six different brain areas as follows: entorhinal cortex and retrosplenial cortex, hilar and CA1 hippocampal cells, nucleus reuniens of the thalamus and habenula. See specific details about FJ/PV double labeling in entorhinal cortex and CA1 pyramidal cells in Figs. 8 and 9.

3. Discussion

One of the main highlights of the H-PILO model is that is more regionally localized, in contrast with the S-PILO model, which is known to have widespread activation of brain circuitry. In the current study, we compared areas with FJ+ cells in both S-PILO and H-PILO models 24 h after SE. We found areas exclusively affected in each group, as well as areas common for both groups (see Table 1). In summary, 34 areas were FJ+ in the S-PILO model, as compared to only 25 areas in the H-PILO model. This result illustrates how extensively S-PILO affects the brain when compared to the H-PILO model. The region with the greatest differences in FJ staining is the thalamus, followed by the hypothalamus, hippocampal formation and amygdala. There were 9 thalamic nuclei stained in the S-PILO model, but only 4 thalamic nuclei stained in the H-PILO one. Interestingly, while these included ventrolateral and centrolateral nuclei of thalamus, those included other nuclei, such as several mediodorsal areas, lateral posterior, dorsal lateral, etc. The only nucleus of the thalamus where there was a staining in both models was the medial mediodorsal thalamic nucleus.

Thalamus is known for communicating cortical areas with most other areas of the CNS, both in afferent and efferent fashion. Functional loops linking cortex and thalamus go back and forth, sometimes trespassing other important movement control areas (e.g. basal ganglia), participating in events such as muscle contraction or behavioral planning and execution. Also, the activation of specific circuitry between thalamus and cortex may lead to consciousness or to various forms of unconsciousness. We certainly do not know what is the meaning of such an ubiquitous activation of thalamus in the S-PILO model, and the activation of only some, and not the same, thalamic nuclei in the H-PILO model. But it may be an indication of a much more restrict activation (considering that neurodegeneration could be a consequence of hyperexcitability/excitotoxicity) of neuronal circuitry in the H-PILO versus the S-PILO models.

Additionally, there were no hypothalamic nuclei stained in H-PILO, whereas there were two of them (medial tuberal and premamillary nuclei, this one considered part of the limbic system) activated in the S-PILO model. With a few exceptions in the most severe seizures we also found lack of staining in CA2 pyramidal cell layer. However, we found lack

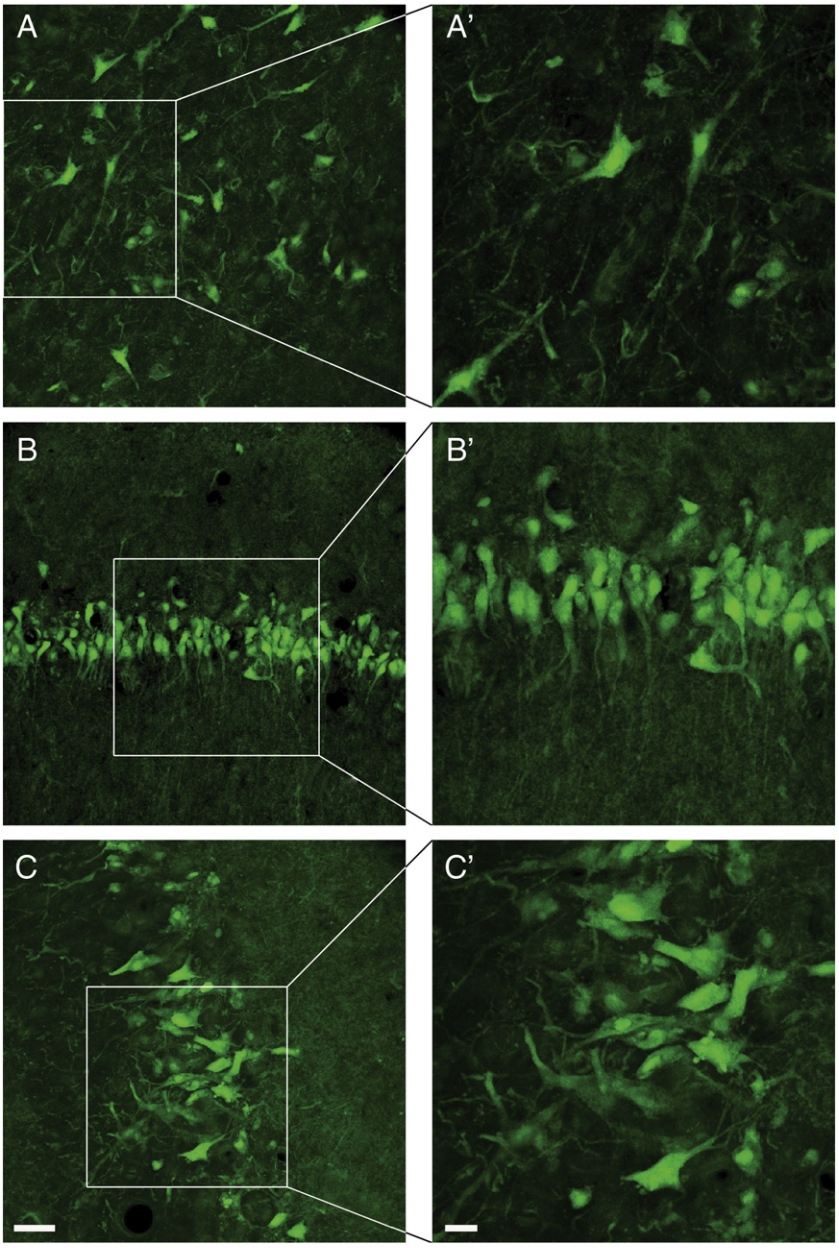

Fig. 5 – Selective FJ+ neurodegeneration after PILO in H-PILO model 24 h after SE. (A) Hilus of dentate gyrus. (A′) Zoom in hilus. (B) CA1. (B′) Zoom in CA1. (C) CA3. (C′) Zoom in CA3. Calibration bars: 25 μm (A–C); 10 μm (A′–C′).

of FJ+ cells in stratum oriens of hippocampal formation, and in the central nucleus of amygdala, in the H-PILO as compared to the S-PILO model. All such areas, in addition to the several other subfields of hippocampal formation and amygdaloid complex that presented FJ+ neurons in both models, were neurodegenerated in the S-PILO model. Thus, our results indicate that there are different circuitries suffering from the hyperexcitability (or at least different cells susceptible to hyperexcitability) when both groups are compared, and these circuitries include not only the thalamic and hypothalamic areas, but also the limbic areas classically implicated in TLE, either human or animal.

In the S-PILO model, alterations were observed in the olfactory cortex, amygdaloid complex, thalamus, neocortex, hippocampal formation, forebrain, and substantia nigra, in agreement with data from Fujikawa (1996, 2005). S-PILO is known to induce a cholinergic–glutamatergic coupling (Turski et al., 1984), which might also be true for the H-PILO model. Pilocarpine is a cholinergic agonist; therefore, we targeted central cholinergic receptors in our models. According to Turski et al. (1984), the evolution and maintenance of SE is glutamatergic. This was confirmed by experiments where the same authors used atropine, immediately after PILO injection, and the animals did not develop SE. On the other hand, if atropine was injected after the onset of SE, the animals did not stop the seizures, proving that SE maintenance is glutamatergic. However, when comparing S-PILO and H-PILO, the differential distribution of neurons undergoing degeneration suggests that the relevant circuitry is different, in spite of seizure generalization during SE.

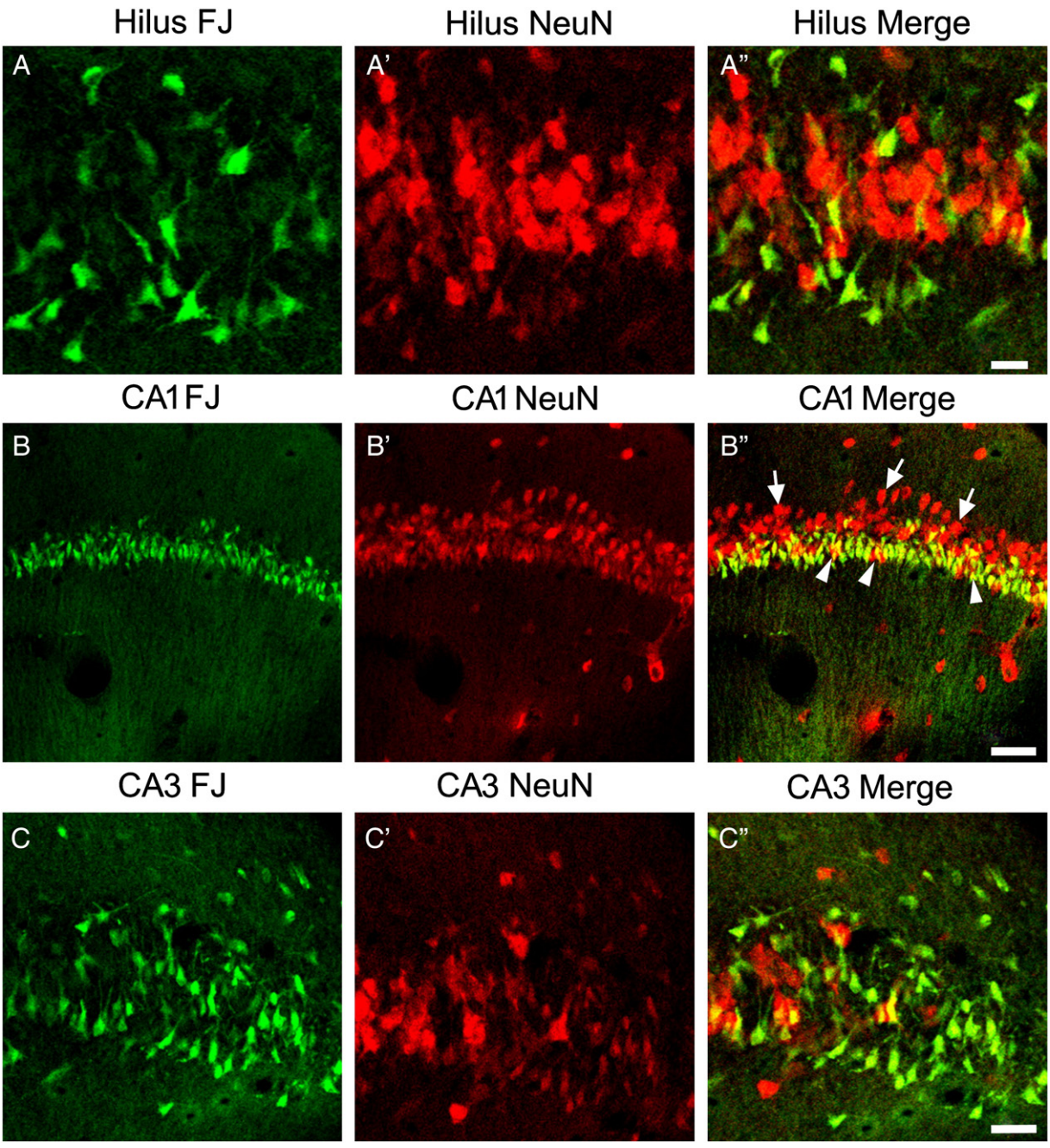

Fig. 6 – Double labeling of FJ/NeuN in the hilus, CA1 and CA3 in the H-PILO model 24 h after SE. Observe the neuronal FJ+ pattern not always coincident with NeuN labeling, indicating selective neurodegeneration. Arrows: NeuN+ cells, arrowhead: FJ/NeuN co-localization. Calibration bars: 25 μm (top panels); 100 μm (middle panels); 50 μm (bottom panels).

Modern neuropathological studies have focused on aspects of neuronal injury, loss of specific neuronal groups and cellular reorganization to address mechanisms of epileptogenesis and the enigma of how specific hippocampal neuronal vulnerabilities and glial proliferation are both the effect and the cause of seizures (Thom, 2009). Thus, although we have observed spread alterations in the rat brain in what concern regional, selective neurodegeneration, we focused a more detailed study on the hippocampal formation.

The pattern of neurodegeneration after SE induced by H-PILO is region- and time-dependent. FJ+ cells were observed in all temporal windows after SE in DG hilus, CA1, and CA3 pyramidal cells, but the number of stained cells differed over time. We observed neurodegeneration early in the DG hilus but later in CA1. According to Poirier et al. (2000), the best time at which to detect neurodegeneration with FJ was 24 h after SE, although the same authors also found neurodegeneration 15 days after the initial insult. In addition, Kubova et al. (2002) found neurodegeneration 3 months after SE induced by PILO and lithium. Although Druga et al. (2010), induced SE in postnatal 12-old-male Wistar rats and detected FJ+ cells in *stratum pyramidale* of CA1.

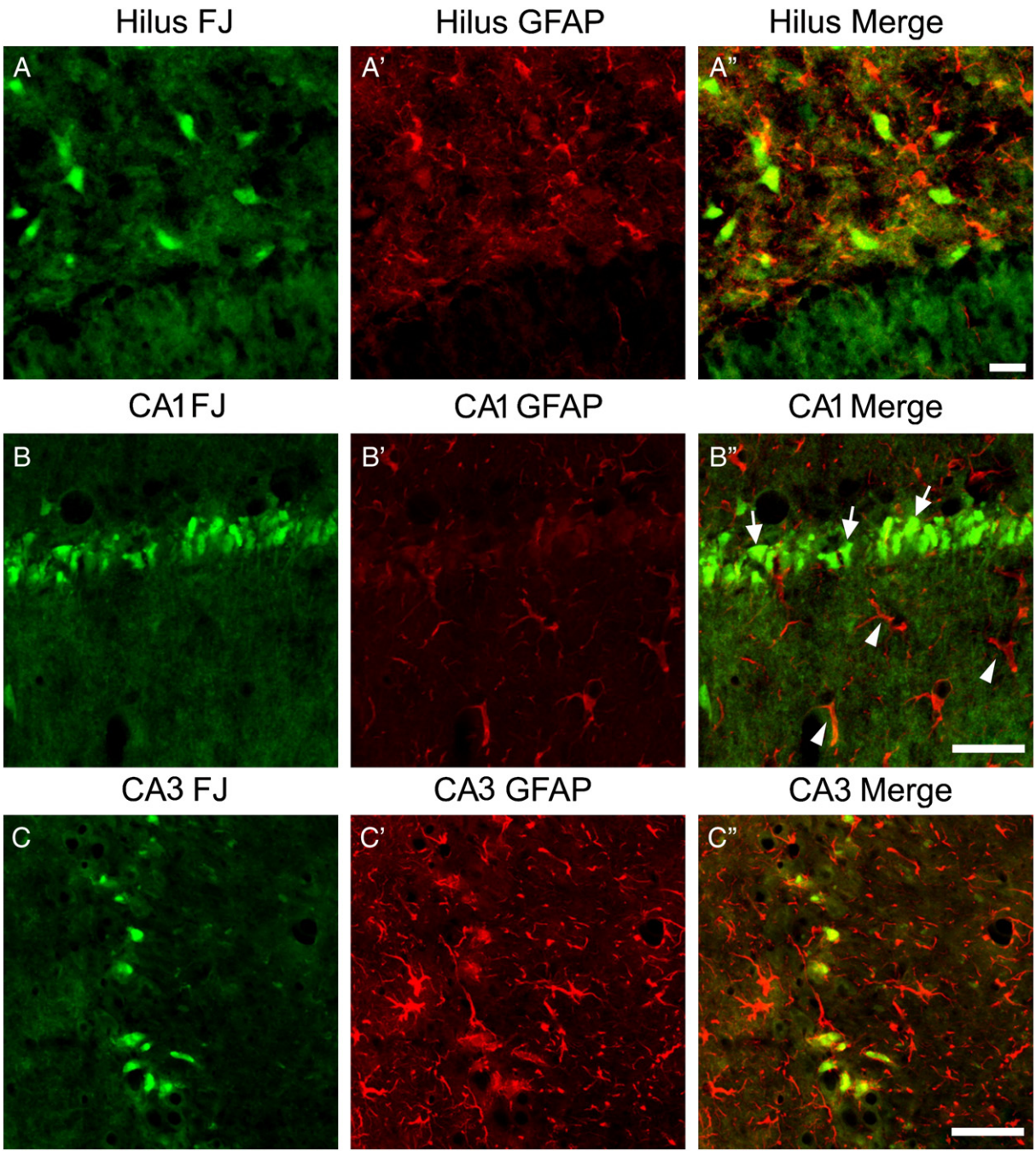

Fig. 7 – Double labeling of FJ/GFAP in the hilus, CA1 and CA3 in the H-PILO model, 24 h after SE. Observe the absence of FJ/GFAP co-localization in the hilus and CA1. Arrows: GFAP+ cells, arrowheads: absence of FJ/NeuN co-localization. Calibration bars: 25 μm (top panels); 100 μm (middle panels); 50 μm (bottom panels).

Activation of excitatory neurons that belong to circuits that include DG–CA3–CA1 can lead to the observed neurodegeneration. We did not find a correlation between seizure severity and cell damage. However, in a few animals that presented the highest scores for SE, we found cell loss in areas thought to be resistant to insults similar to PILO, including CA2 and the granule cell layer of DG. According to Baimbridge and Miller (1982), such areas have high amounts of calcium binding proteins when compared with CA1 or CA3, which could explain their relative resistance to neurodegeneration. Furthermore, the excessive activation of NMDA receptors in these hyperexcitable circuits can increase intracellular calcium, inducing mechanisms that lead to several biochemical processes resulting in cell death (McNamara, 1994). FJ+ cells are found mostly after prolonged seizures such as those observed in SE (Schmued et al., 1997). Because our animals were kept in SE for 90 min, these seizures are long enough to induce neurodegeneration.

While some reports have shown that FJ can stain glial cells in the cerebral cortex of primates (Colombo and Puissant,

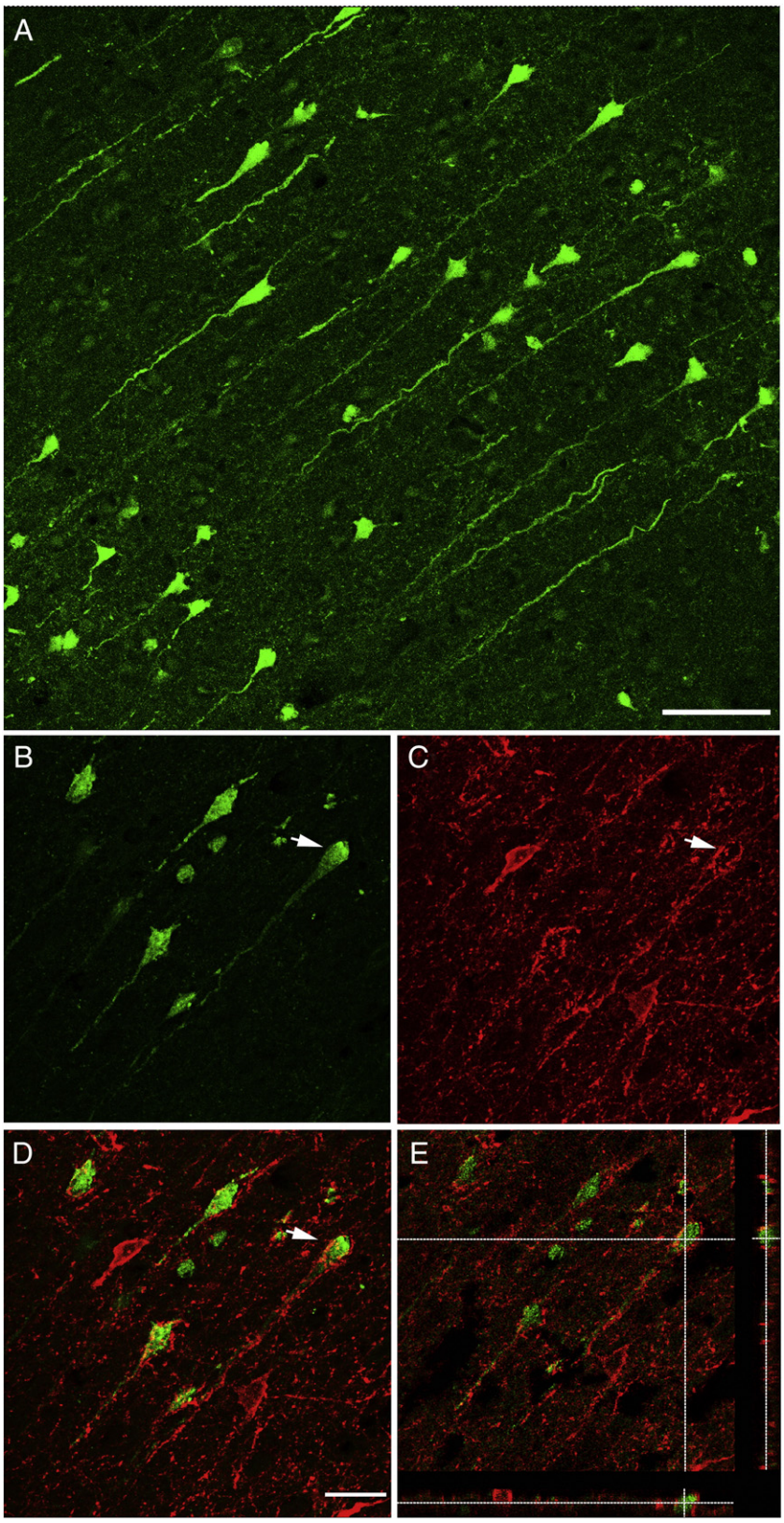

Fig. 8 – FJ/PV double labeling in the H-PILO model, 24 h after SE. (A) FJ+ neurodegeneration in deep layers of entorhinal cortex, including typical "corkscrew"-like degeneration of dendrites. (B) PV+ cells and PV+ processes. (C) Absence of FJ/PV co-localization and clear-cut PV+ labeling surrounding the FJ+ delineated neuronal structure. (D) Merged image of (B) and (C). (E) Orthogonal imaging of (D) evidencing the absence of FJ/PV co-localization. Calibration bars: 75 μm (A); 25 μm (B–D).

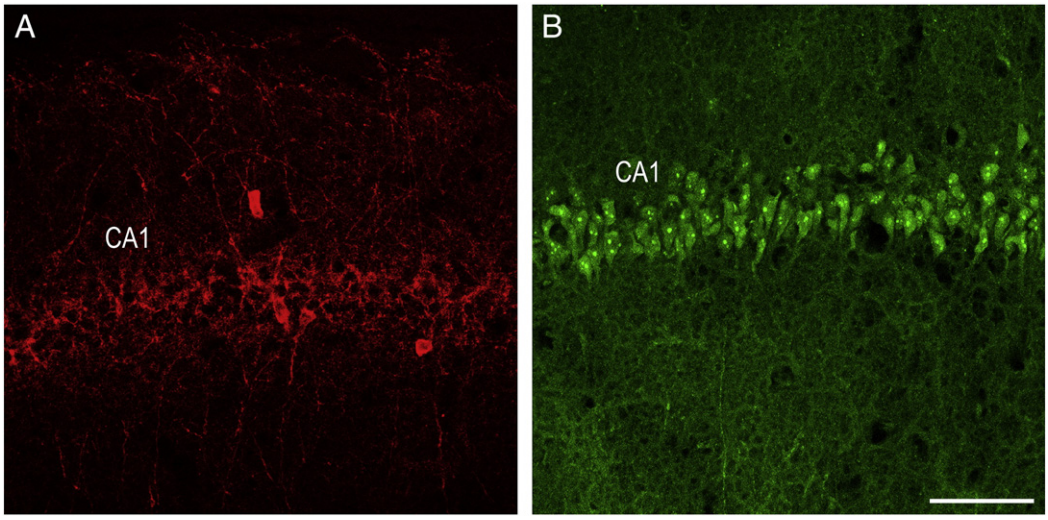

Fig. 9 – Labeling of FJ/PV in the H-PILO model 24 h after SE. Although this is an observation of adjacent sections, the pattern and amount of FJ and PV labeling are strongly suggestive of absence of FJ/PV co-localization in CA1 pyramidal cells. (A) PV+ cells. (B) FJ+ cells. Calibration bar: 75 μm (A and B).

2002), Poirier et al. (2000) showed that cells labeling for GFAP do not co-localize with FJ. During all the quantitative analysis in this study, we used sections with FJ histochemistry only, without double staining for NeuN or GFAP. Therefore, we counted only FJ+ cells that had typical neuronal anatomy, including interneurons (hilus of DG) and pyramidal cells (CA3 and CA1). In the double labeling studies, we found partial co-localization between FJ+ neurons with GFAP. Whether or not the lack of immunoreactivity to NeuN represents a true loss of neurons (Igarashi et al., 2001; Sugawara et al., 2002) or simply a transient phenomenon of reduced antigenicity, as suggested by others (Collombet et al., 2006; Mullen et al., 1992; Unal-Cevik et al., 2004), is still controversial. As we did not use antigenic retrieval in our protocol, we cannot argue for one or another. Nonetheless, we found decreased number of NeuN+ cells in the cerebral cortex of patients suffering from traumatic brain injury (Blümcke et al., 2009). We might suggest that NeuN labeling can be seen as a marker of healthy neurons, whereas FJ+ neurons are cells undergoing a degenerative process.

Other characteristics of the H-PILO model are improvements in comparison to the S-PILO model, as has been previously shown in our laboratory (Furtado et al., 2002). For instance, H-PILO conserves essential features such as the presence of spontaneous recurrent seizures and neo-Timm-positive mossy fiber sprouting. Advantages of the H-PILO model include near zero mortality (as compared to about 70% observed in the S-PILO model), development of SE in more than 90% of animals (as compared to about 50% in the S-PILO model), the possible induction of SE by the activation of more restricted areas of the brain (see Table 1), no need for pre-treatment with peripheral muscarinic receptor blockers, and faster recovery after diazepam injection. Indeed, S-PILO animals demand intensive care for a couple of days after recovery from SE, which is not necessary with the H-PILO model. Nonetheless, there are some disadvantages of the H-PILO model, such as the necessity of stereotaxic surgery in all animals, which obviously increases the amount of time spent on preparation for experiments. Another disadvantage is that a mechanical lesion occurs, which is caused by the cannula in the nervous tissue on and above the hippocampal area that is chemically stimulated. However, this mechanical effect is controlled in independent groups of cannula-implanted animals without microinjections and with cannula-implanted animals treated only with vehicle. Even though the above disadvantages exist, it is our belief that all the previously mentioned advantages justify the additional effort necessary for induction of the H-PILO model. Table 2 compares the pros and cons listed in this comparative discussion of the S-PILO and H-PILO models. Additional information was taken from features already described for the H-PILO model in Furtado et al. (2002).

In addition to the advantages shown by the H-PILO protocol, the time course of the FJ+ neurodegeneration is clear-cut and appears to follow the natural trisynaptic pathway (DG-CA3-CA1). Although the time course of neurodegeneration being coincident with the trisynaptic pathway might be an epiphenomenon, we cannot exclude the possibility that it is a reflection of some mechanism- and time-related pathological process. For example, Sloviter et al. (1996) found a similar sequence of hippocampal cell death in the repetitive, intermittent perforant path stimulation model of epilepsy. Furthermore, a different time course of neurodegeneration seen in each specific region, associated with behavioral seizure severity during SE, has also been evaluated in the model of self-sustained SE induced by electrical stimulation of the amygdala (Tilelli et al., 2005).

Interestingly, several articles have been published in the last few years that suggest differential histopathology of hippocampal formation in distinct patients presenting with TLE (Silva et al., 2007; Blümcke et al., 2009; Thom, 2009). Such studies rely on anatomical pieces of temporal lobe, focusing their evaluations in the hippocampal formation, not allowing for a better comparability of our results and theirs (as we looked at most prosencephalon and diencephalon areas). Nonetheless, there is histopathological evidence from human specimens that TLE might present with more than

Table 2 – Comparison between the S-PILO and H-PILO TLE models. Data from the current study and from Furtado et al. (2002).

	S-PILO	H-PILO
Spontaneous recurrent seizures	Yes	Yes
Mossy fiber sprouting	Yes	Yes
Mortality after SE induction	70%	0–10%
SE induction after drug injection	50%	90–100%
Damaged areas after SE induction	Broad	Restricted
Pre-treatment with peripheral muscarinic receptor blocker	Yes	No
Recovery after SE rescue	Days	Hours
Need for stereotaxic surgery	No	Yes
Mechanical lesion produced by cannula	No	Yes

one pattern of plastic, pathologic neural substrate. The mentioned articles show different patterns of granular cells of the DG dispersion (cell loss with thinning, dispersion with invasion of molecular layer, clusters of ectopic cells and bilaminar architecture). Thus, there is a need to not disregard that a laminar subfield cell suffering/degeneration could, for example, lead to cell loss with layer thinning or could represent an initial phase of bilaminar function, both patterns described for granular cell layer of DG in human TLE.

Along these lines, one striking finding worth pursuing in future experiments is the selective, laminar FJ+ pattern of neurodegeneration after H-PILO. This pattern is particularly notable in area CA1 (see Fig. 7B). We believe that this laminar pattern of neurodegeneration is dependent on the specific hodology (i.e., afferents/efferents) of the various layers of the hippocampus, because trans-synaptic anterograde or retrograde interactions can explain distant and selective neurodegenerated targets (Ramirez, 2001; Witter and Amaral, 1991, 2004, see details below). In our specific case, the FJ+ laminar pattern of neurodegeneration in the stratum pyramidale/stratum radiatum (SR) transition and the NeuN+ labeling (preserved cells) in the stratum pyramidale/stratum oriens transition are quite suggestive of entorhinal cortical (EC) neurodegeneration preceding that of CA1. It will be particularly interesting to verify whether or not the known rostro-lateral EC-CA1 projections studied with anterograde tracers by Witter et al. (1988) might be the source of current laminar neurodegeneration.

Jinno and Kosaka (2009) have recently shown that, after electroconvulsive shock, there is a circuit-dependent alteration of the expression of two isoforms of glutamic acid decarboxylase (GAD). The authors describe that the expression levels of GAD65 in GABAergic neurons were specifically increased in layers receiving afferents from EC (i.e., SR/stratum lacunosum moleculare (SLM) of the CA1 region and molecular layer of DG). An additional clear-cut example of this long-distance plasticity is the model of compensatory axonal temporo-dentate sprouting consequent to electrolytic lesions of EC (Ramirez et al., 1999). Further sources of neurodegeneration still to be proven in the H-PILO model might be those associated with amygdala–hippocampus connections, also based upon known connectivity between these two regions (Witter and Amaral, 2004).

One striking structural phenomenon was the FJ/PV double labeling in the entorhinal cortex (see Fig. 8). At the same time there is a distinct FJ+ labeling of the whole neuronal soma and dendritic/axonal processes, there is concomitant PV+ pericellular labeling, making a sort of shell of multiple contacts onto the FJ+ delineated structure. Fig. 8A highlights in the FJ+ images of entorhinal cortex the typical "corkscrew"-like degeneration of dendrites, quite similar to the one already described with other kinds of brain insults (de Olmos et al., 1994).

It is curious that Arellano et al. (2004) have shown very similar pericellular patterns of PV+ labeling in epileptic tissue from patients with TLE. However, it seems to us that this is the first time there is a description of FJ+/PV+ double labeling with this aberrant but singular pattern of embracing PV terminals onto a FJ+ neurodegenerating cell. The results from cortical FJ+ cells highlight the importance of analysis of extra-hippocampal regions, which in this case are probably responding for the absence of correlation between hippocampal damage and seizure severity." The analysis of double labeling in CA1 showed no co-localization of FJ and PV (see Fig. 9).

Finally, based on those data and our observations, we believe that (1) we presented here evidence that the neural substrates for SE originated from S-PILO and H-PILO models are partially superposed but nonetheless present important regional differences; (2) as human TLE can show similar signs and symptoms with different neural substrates, different models of TLE could and actually should be used to investigate the neurobiology of epilepsy and epileptogenesis, as they probably model distinct neuropathologies subjacent to the epileptic phenomenon and (3) H-PILO model is a new animal model for TLE, that is distinct histopathologically from S-PILO, besides adding desirable characteristics, such as higher proportion of animals that develop SE and do not perish from it, therefore could add information for new insight into the physiopathology of TLE.

4. Conclusion

Our data suggest that the H-PILO model is a reliable new tool for the study of neurodegeneration and epilepsy consequent to SE. The differential neurodegeneration pattern observed in our study, when compared to the S-PILO model, shows that the H-PILO model can be useful for the understanding of epilepsy and epileptogenesis in a complementary way to current models of temporal lobe seizures. The regionally (hilus, CA3, and CA1) selective kinetics (24, 48 and 168 h) of FJ+ neurodegeneration and low mortality are highlights of the H-PILO model.

There is also a selective kinetics of FJ+ cells in the hippocampus after SE induced by H-PILO, with no association with the severity of seizures, probably as a consequence of the extra-hippocampal damage. These data point to SE induced by H-PILO as a low-mortality model of TLE, with regional spatial and temporal patterns of FJ staining.

5. Experimental procedures

5.1. *Animals*

Adult male Wistar rats ($n=46$, 240–340 g), from the main vivarium of the Ribeirão Preto Campus at the University of São Paulo, were used. Animals were individually housed in cages

in a controlled environment with constant temperature (21 °C) and a 12/12 h light/dark cycle, with lights on at 07:00 AM and lights off at 07:00 PM. Access to food and water was unlimited. All procedures were conducted in accordance with the guidelines set by the Brazilian College of Animal Experimentation (COBEA) and were approved by the Ribeirão Preto School of Medicine Commission on Ethics ton Animal Experimentation (CETEA; protocol # 195/2005).

5.2. *Behavioral analysis*

Animals from control and experimental groups were individually placed in acrylic cages and their behavior was recorded on videotapes for up to 3 h. For seizure severity scoring, the 90-min time window was split into 18 windows of 5 min each, from which the maximum seizure severity (Pinel and Rovner, 1978; Racine, 1972) was taken as the representative of that window (Tilelli et al., 2005). All animals were divided into groups according to the seizure severity score most prevalent during the 90 min of SE: (A) class 1, (B) class 2, (C) class 3, (D) class 4, and (E) class 5. In order to be classified in a specific group, animals had to spend more than 50% of the time in a certain seizure class. For example, animals classified as class A stayed between class 1 and 2 for more than 50% of the 18 recorded windows.

5.3. *Surgery*

Animals were deeply anesthetized with 10 ml/kg of tribromo ethanol (2.5%; Aldrich Chemical Inc., Milwaukee, WI, USA), followed by veterinary pentabiotic, 1 ml/kg (Fort Dodge, Campinas, SP, Brazil) to avoid infection. Cannulae were implanted in specific stereotaxic coordinates (Paxinos and Watson, 1996): hilus of the DG: –6.30 mm anterior–posterior (AP, reference; bregma), 4.50 mm medial–lateral (ML, reference: sagittal sinus), –4.50 mm dorsal–ventral (DV, reference: *dura mater*).

5.4. *Intrahippocampal microinjections*

Male adult Wistar rats were implanted and after 7 days submitted to the experimental protocol. Animals were gently restrained during the H-PILO microinjection. A 5 μl syringe (Hamilton Company, Reno, NV, USA) connected to a microinjection pump (Harvard Apparatus PHD 2000, Holliston, MA, USA) was used. The total injected volume was 1 μl, dose of 2.4 mg/μl at a speed of 0.5 μl/min. The experimental groups (n=28) were injected with PILO, and the control groups (n=18) were injected with saline (0.9%; 1 μl). All animals that had SE were rescued with diazepam (DZP; 5 mg/kg; ip), 90 min after SE establishment. Animals that did not have SE and control groups were also injected with DZP in the same conditions.

5.5. *Systemic PILO injection*

Animals were injected intra-peritoneally with methylscopolamine (2 mg/kg), followed after 30 min by PILO in a dose of 320 mg/kg and were observed as in the previous groups. Control group received saline instead of PILO in a similar volume. All animals that had SE were rescued with DZP (5 mg/kg; ip), 90 min after SE establishment. Animals that did not have SE and control groups were also injected with DZP in the same conditions.

5.6. *Histology*

Animals were injected with an overdose of sodium thiopental and were perfused transaortically with 0.1 M PBS and 4% paraformaldehyde solution in PBS. Afterwards, the brains were removed, cryoprotected with sucrose 20%, frozen in isopentanol/dry ice, and stored at –20 °C. Sections were then cut (30 μm thickness) with the aid of a cryostat (Microm HM-505-E, Microm International, Walldorf, Germany) and were processed for Nissl and FJ staining.

5.7. *FJ staining procedure*

For comparison of whole brain between models (H-PILO versus S-PILO), S-PILO animals were perfused 24 h after the PILO injection (n=6).

Animals from the H-PILO group were perfused at 12 (n=15), 24 (n=13) or 168 h (7 days; n=18) after SE. We used FJ histochemistry as described by Schmued et al. (1997). For better quality and conservation of tissue, sections were mounted directly inside the cryostat onto gelatin coated slides. Slides were subsequently stored in a freezer at –20 °C.

FJ staining was performed as follows: tissue was immersed in 100% ethanol for 3 min, followed by 1 min in 70% ethanol and 1 min in distilled water. After this step, slides were transferred to a solution of 0.06% potassium permanganate for 15 min and were gently shaken on a rotating platform. Slides were rinsed three times for 1 min in distilled water and were then transferred to the FJ staining solution and were gently shaken for 30 min. The 0.0001% working solution of FJ was prepared by adding 1 ml of stock FJ solution (0.01%) to 99 ml of 0.1% acetic acid in distilled water. After staining, sections were rinsed three times (1 min) in distilled water and slides were coverslipped.

5.8. *Mapping FJ+ areas, neuronal-specific nuclear protein (NeuN), glial fibrillary acidic protein (GFAP) and parvalbumin (PV) immunohistochemistry and cell counting*

Slides from animals from both H-PILO and S-PILO models in the 24 h groups were analyzed separately by two independent observers. Areas where FJ+ cells were seen were annotated. FJ+ cells were counted only when they displayed typical neuronal anatomy, including interneurons (hilus of DG) and pyramidal cells (CA3 and CA1). All areas that contained FJ+ cells in at least one animal in a group were included in Table 1. In the double labeling studies, FJ/NeuN, FJ/GFAP, FJ/PV cells were qualitatively described as present or absent. Areas analyzed ranged from –2.12 to –6.30 mm to Bregma, according to the Paxinos and Watson (1996) Atlas.

5.9. *Image analysis*

All images were digitized using an Optronics CCD camera 750L (Santa Barbara, CA, USA) connected to an Olympus microscope BX-60 (Olympus, Melville, NY, USA).

5.10. *Confocal imaging acquisition*

Hipocampal sections were examined with Leica TCS SP5 confocal microscope (Leica Microsystems, Mannheim, Germany). Confocal images of a single optical plane (1 μm thick) were obtained using appropriate emission and excitation wavelengths. The argon–krypton laser was used to excite the FJ, GFAP and PV) and neuronal-specific nuclear protein (NeuN); Alexa 594 fluorochrome, at 488 and 594 nm, respectively. Fluorescence signal cross-talk among the different channels was avoided by setting image-acquisition parameters with individually labeled sections. For confocal imaging, laser attenuation, pinhole diameter, photomultiplier sensitivity and offset were kept constant for every set of experiments.

5.11. *NeuN, GFAP and PV immunohistochemistries*

The immunohistochemistry assays were done in free floating tissue and the protocol used for detection of NeuN, GFAP and PV antigens was the same, with only alteration of primary antibodies. The following primary antibodies were used: mouse-∞-NeuN (MAB377; Chemicon International, Inc; 1:700), rabbit-∞-GFAP (Chemicon International, Inc; 1:250) and mouse -∞- PV (Sigma, Inc; 1:5000) secondary antibodies: goat-∞-rabbit and goat-∞-mouse, alexa 594 (Molecular Probes; 1:2000). Briefly, the immunohistochemistry protocol begins with three baths of 3–5 min in PBS 10 mM, followed by 5 min bath with glycine 0,1 M in PBS. Three 5-min PBS baths were made in order to remove the excess of glycine. Additional three PBS baths were done containing Triton X-100 (Sigma) 0.1% (PBS-T). Sections were incubated for 2 h, under mild agitation, in PBS-T containing 3% of bovine serum albumin (BSA), fraction V (Sigma). Sections were then placed with each primary antibody diluted in BSA and left under mild agitation until the next day, completing 12–22 h of incubation. The second day of the protocol was initiated with eight baths of 3–5 min in PBS followed by incubation with the secondary antibody diluted in BSA, for 1–1.5 h. The sections were washed again in PBS six times 3–5 min. Finally the sections were transferred to gelatinized slides and mounted with Fluoromont (EMS).

5.12. *Double labeling of FJ+ cells with either NeuN, GFAP or PV*

FJ/NeuN and FJ/GFAP double labelings were made after separated immunohistochemistries for NeuN and GFAP. The FJ histochemistry begins with a 2 min distilled water bath, followed by 5 min of potassium permanganate, under mild agitation. The excess of permanganate was removed with 1 bath of distilled water, followed with the incubation with FJ for 10 min, in the same dilution conditions described above in the FJ protocol. After this, an additional 1 min bath of distilled water was made and finally the sections received a xylol bath and were mounted with Entellan.

5.13. *Cell counting*

Cell counting was done with ImageJ (Wayne Rasband; Research Services Branch, National Institute of Mental Health, Bethesda, MD, USA).

In the H-PILO model we determined the number of cells in three hippocampal regions: CA1, CA3 and DG hilus. These regions were selected because they are sensitive to the neurodegeneration process. For the quantification of neurodegenerating cells we sampled up to 10 areas, in three different coordinates of the hippocampus (AP –2.56 mm; AP –3.30 mm and AP –6.30 mm), according to Paxinos and Watson (1996). The selected areas are shown in Fig. 1. All the cells were counted in the contralateral hippocampus, because animals injected with PILO develop a scar surrounding the microinjection site. Those scars are due to mechanical lesions caused by cannulae and local action of PILO. The severity of the scar is reduced in control animals.

5.14. *Statistical analysis*

For statistical analysis we used SigmaStat Software (v. 3.1, Aspire Software Int., Ashburn, VA, USA). To determine the temporal distribution of FJ+ cells, after a normality test determined that the samples were not normally distributed, we performed the one-way ANOVA Kruskal–Wallis test, followed by Dunn's post-hoc test. To verify if there was a correlation between degree of neurodegeneration and severity of SE, we used Pearson's correlation test. $P \leq 0.05$ was considered statistically significant.

Acknowledgments

We thank FAPESP (Grant number: 2007/50261-4), FAPESP-Cinapce (Grant number 2005/56447-7); CAPES-PROEX, PRONEX, CNPq and FAEPA/HC-FMRP-USP for financial support. We thank also Franco Rossetti for statistical analysis and Marcia Graeff for technical support with the confocal microscopy. We thank also Dr. Benedito Honório Machado for his support to this project. O.W.C. held a CAPES-Brazil MSc Fellowship. N.G.C. holds a CNPq-Brazil Research Fellowship.

REFERENCES

Arellano, J.I., Muñoz, A., Ballesteros-Yañez, I., Sola, R.G., DeFelipe, J., 2004. Histopathology and reorganization of chandelier cells in the human epileptic sclerotic hippocampus. Brain 127, 45–64.

Baimbridge, K.G., Miller, J.J., 1982. Immunohistochemical localization of calcium-binding protein in the cerebellum, hippocampal formation and olfactory bulb of the rat. Brain Res. 245, 223–229.

Blümcke I., Kistner I., Clusmann H., Schramm J., Becker A.J, Elger C.E., Bien C.G., Merschhemke M., Meencke H.J., Lehmann T., Buchfelder M., Weigel D., Buslei R., Stefan H., Pauli E., Hildebrandt M., 2009. Towards a clinico-pathological classification of granule cell dispersion in human mesial temporal lobe epilepsies.

Collombet, J.M., Masqueliez, C., Four, E., Burckhart, M.F., Bernabe, D., Baubichon, D., Lallement, G., 2006. Early reduction of NeuN antigenicity induced by soman poisoning in mice can be used to predict delayed neuronal degeneration in the hippocampus. Neurosci. Lett. 398, 337–342.

Colombo, J.A., Puissant, V.I., 2002. Fluoro Jade stains early and reactive astroglia in the primate cerebral cortex. J. Histochem. Cytochem. 50, 1135–1137.

Druga, R., Mares, P., Kubová, H., 2010. Time course of neuronal damage in the hippocampus following lithium-pilocarpine status epilepticus in 12-day-old rats. Brain Res. 8 (1355), 174–179.

Fujikawa, D.G., 2005. Prolonged seizures and cellular injury: understanding the connection. Epilepsy Behav. 7, S3–S11.

Fujikawa, D.G., 1996. The temporal evolution of neuronal damage from pilocarpine-induced status epilepticus. Brain Res. 725, 11–22.

Furtado, M.A., Braga, G.K., Oliveira, J.A., Del, V.F., Garcia-Cairasco, N., 2002. Behavioral, morphologic, and electroencephalographic evaluation of seizures induced by intrahippocampal microinjection of pilocarpine. Epilepsia 43 (Suppl. 5), 37–39.

Igarashi, T., Huang, T.T., Noble, L.J., 2001. Regional vulnerability after traumatic brain injury: Gender differences in mice that overexpress human copper, zinc superoxide dismutase. Exp. Neurol. 172, 332–341.

Jinno, S., Kosaka, T., 2009. Neuronal circuit-dependent alterations in expression of two isoforms of glutamic acid decarboxylase in the hippocampus following electroconvulsive shock: a stereology-based study. Hippocampus 11, 1130–1141.

Kubova, H., Druga, R., Haugvicova, R., Suchomelova, L., Pitkanen, A., 2002. Dynamic changes of status epilepticus-induced neuronal degeneration in the mediodorsal nucleus of the thalamus during postnatal development of the rat. Epilepsia 43 (S5), 54–60.

McNamara, J.O., 1994. Cellular and molecular basis of epilepsy. J. Neurosci. 14, 3413–3425.

Mohapel, P., Ekdahl, C.T., Lindvall, O., 2004. Status epilepticus severity influences the long-term outcome of neurogenesis in the adult dentate gyrus. Neurobiol. Dis. 15, 196–205.

Mullen, R.J., Buck, C.R., Smith, A.M., 1992. NeuN, a neuronal specific nuclear protein in vertebrates. Development 116, 201–211.

de Olmos, J.S., Beltramino, C.A., de Olmos de Lorenzo, S., 1994. Use of an amino-cupric-silver technique for the detection of early and semiacute neuronal degeneration caused by neurotoxicants, hypoxia and physical trauma. Neurotoxicol. Teratol. 16, 545–561.

Paxinos, G., Watson, C., 1996. The rat brain in stereotaxic coordinates. Academic Press, Inc.

Pinel, J.P., Rovner, L.I., 1978. Experimental epileptogenesis: kindling-induced epilepsy in rats. Exp. Neurol. 58, 190–202.

Poirier, J.L., Capek, R., De, K.Y., 2000. Differential progression of Dark Neuron and Fluoro-Jade labelling in the rat hippocampus following pilocarpine-induced status epilepticus. Neuroscience 97, 59–68.

Racine, R.J., 1972. Modification of seizure activity by electrical stimulation. II. Motor seizure. Electroencephalogr. Clin. Neurophysiol. 32, 281–294.

Ramirez, J.J., 2001. The role of axonal sprouting in functional reorganization after CNS injury: lessons from the hippocampal formation. Restor. Neurol. Neurosci. 19 (3–4), 237–262.

Schmued, L.C., Albertson, C., Slikker, W., 1997. Fluoro-Jade: a novel fluorochrome for the sensitive and reliable histochemical localization of neuronal degeneration. Brain Res. 751, 37–46.

Shorvon, S.D., 2000. Handbook of epilepsy treatment. Blackwell Science, London.

Silva, A.V., Houzel, J.C., Croaro, I., Targas Yacubian, E.M., Stavale, J.N., Centeno, R.S., Cavalheiro, E.A., 2007. Granular cell dispersion and bilamination: two distinct histopathological patterns in epileptic hippocampi? Epileptic Disord. 9 (4), 438–442.

Sloviter, R.S., Dean, E., Sollas, A.L., Goodman, J.H., 1996. Apoptosis and necrosis induced in different hippocampal neuron populations by repetitive perforant path stimulation in the rat. J. Comp. Neurol. 366, 516–533.

Sugawara, T., Lewen, A., Noshita, N., Gasche, Y., Pak, H.C., 2002. Effects of global ischemia duration in neuronal, astroglial, oligodendroglial, and microglial reactions in the vulnerable hippocampal CA1 subregion in rats. J. Neurotrauma 19, 85–98.

Thom, M., 2009. Hippocampal sclerosis: progress since Sommer. Brain Pathol. 19 (4), 565–572.

Tilelli, C.Q., Del, V.F., Fernandes, A., Garcia-Cairasco, N., 2005. Different types of status epilepticus lead to different levels of brain damage in rats. Epilepsy Behav. 7, 401–410.

Turski, L., Cavalheiro, E.A., Czuczwar, S.J., Turski, W.A., Kleinrok, Z., 1987. The seizures induced by pilocarpine: behavioral, electroencephalographic and neuropathological studies in rodents. Pol. J. Pharmacol. Pharm. 39, 545–555.

Turski, W.A., Cavalheiro, E.A., Bortolotto, Z.A., Mello, L.M., Schwarz, M., Turski, L., 1984. Seizures produced by pilocarpine in mice: a behavioral, electroencephalographic and morphological analysis. Brain Res. 321, 237–253.

Unal-Cevik, I., Kilinc, M., Gursoy-Ozdemir, Y., Gurer, G., Dalkara, T., 2004. Loss of NeuN immunoreactivity after cerebral ischemia does not indicate neuronal cell loss: a cautionary note. Brain Res. 1015, 169–174.

Witter, M.P., Amaral, D.G., 1991. Entorhinal cortex of the monkey. V. Projections to the dentate gyrus, hippocampus, and subicular complex. J. Comp. Neurol. 15 307 (3), 437–459.

Witter, M.P., Griffioen, A.W., Jorritsma-Byham, B., Krijnen, J.L., 1988. Entorhinal projections to the hippocampal CA1 region in the rat: an underestimated pathway. Neurosci. Lett. 85 (2), 193–198.

Witter, M.P., Amaral, D.G., 2004. The hippocampal region, In: Paxinos, G. (Ed.), The Rat Brain, 3rd edition. Elsevier Academic Press, San Diego, CA, US, pp. 637–703.